N-WASP activation by a β1-integrin-dependent mechanism supports PI3K-independent chemotaxis stimulated by urokinase-type plasminogen activator

Justin Sturge[1], Jocelyne Hamelin[2] and Gareth E. Jones[1,*]

[1]The Randall Centre for Molecular Mechanisms of Cell Function, New Hunt's House, King's College London, Guy's Campus, London SE1 1UL, UK
[2]INSERM U461, F-92296, France
*Author for correspondence (e-mail: gareth.jones@kcl.ac.uk)

Accepted 12 November 2001
Journal of Cell Science 115, 699-711 (2002) © The Company of Biologists Ltd

Summary

Urokinase-type plasminogen activator (uPA)-uPA receptor (uPAR) and epidermal growth factor (EGF)-EGF receptor (EGFR) expression is highly correlated with breast cancer metastasis. Phosphoinositide 3-kinase (PI3K), small Rho GTPases, such as Cdc42 and Rac1, and neuronal Wiskott Aldrich syndrome protein (N-WASP) are key effectors that regulate dynamic changes in the actin cytoskeleton and cell migration. uPA- and EGF-stimulated chemotaxis, cytoskeletal rearrangements and activation of Cdc42, Rac1 and N-WASP were studied in the highly metastatic human breast cancer cell line MDA MB 231. These studies reveal that divergent signalling occurs downstream of PI3K. The activity of PI3K was not necessary for uPA-induced chemotactic responses, but those induced by EGF were entirely dependent upon PI3K. Furthermore, PI3K-independent chemotactic signalling by uPA was shown to involve disruption of an interaction between β_1-integrins and N-WASP and translocation of N-WASP to the actin cytoskeleton.

Keywords: Cell migration, Chemotaxis, Phosphoinositide 3-kinase, Rho GTPases, Actin, Cytoskeleton

Introduction

Chemotaxis is an elaborate process characterised by the migration of cells towards the high concentration point of a chemoattractant gradient (Jones, 2000), and plays an important role in metastasis (Muller et al., 2001; Liotta and Kohn, 2001). Phosphatidylinositol 3-kinase (PI3K) has been suggested to be pivotal for the generation of cell polarity and promotion of chemotaxis (Haugh et al., 2000; Hirsch et al., 2000; Li et al., 2000; Vanhaesebroeck et al., 1999).

The activation of guanine nucleotide exchange factors (GEFs) by 3′ phosphoinositides produced by PI3K (Han et al., 1998) and attenuation of cytoskeletal rearrangements by targeted inhibition of specific PI3K p110 catalytic subunits (Hill et al., 2000; Vanhaesebroeck et al., 1999) suggest that increased PI3K activity switches the small Rho GTPases into an active state. In particular, the small Rho GTPases Cdc42, Rac1 and RhoA have well established roles in regulating the complex cytoskeletal dynamics that drive cell migration (Kjoller and Hall, 1999; Ridley et al., 1999; Schmitz et al., 2000). Cdc42 stimulates microspike formation, polarisation and controls cell directionality (Allen et al., 1997; Allen et al., 1998; Kozma et al., 1995; Nobes and Hall, 1999). Rac1 stimulates lamellipodia formation, membrane ruffling and increases migratory speed (Allen et al., 1997; Allen et al., 1998; Nobes and Hall, 1999; Ridley et al., 1992; Rottner et al., 1999). RhoA induces formation of stress fibres and focal adhesions and regulates cell contractility (Machesky and Hall, 1997; Nobes and Hall, 1995; Nobes and Hall, 1999; Ridley and Hall, 1992; Rottner et al., 1999). In actively migrating cells, Cdc42 and Rac both regulate the formation of focal complexes (small integrin clusters at the edge of lamellipodia that are distinct from the large focal adhesions formed by RhoA in adherent and stationary cells) (Adams, 2001; Nobes and Hall, 1995).

The identification of Wiskott Aldrich syndrome protein (WASP) family members as downstream molecular binding targets for small Rho GTPases represents a direct link between these effectors and reorganisation of the actin cytoskeleton (Millard and Machesky, 2001; Mullins and Machesky, 2000; Takenawa and Miki, 2001). WASP expression is restricted to haematopoietic cells, but its homologue N-WASP is expressed ubiquitously (Kolluri et al., 1996; Miki et al., 1998; Rohatgi et al., 1999; Symons et al., 1996). A model for N-WASP activation by Cdc42 has been conceived from in vitro studies. Binding of Cdc42 to the GDB/CRIB (GTPase binding domain/Cdc42 and Rac interactive binding) region disrupts an autoinhibitory interaction between the N- and C-termini of N-WASP. The newly exposed VCA (Verprolin homology, Cofilin homology, acidic region) domain binds to actin and the Arp2/3 complex to promote actin nucleation and formation of protrusive structures, most notably microspikes/filopodia and lamellipodia (Kim et al., 2000; Millard and Machesky, 2001; Takenawa and Miki, 2001). The polyproline region of WASP and N-WASP binds to SH3 domains of numerous signalling molecules (Fawcett and Pawson, 2000; Takenawa and Miki, 2001), including the p85α regulatory subunit of PI3K (Banin et al., 1996; Finan et al., 1996). So far no function has been assigned to the direct interaction of p85α with N-WASP; however it is likely that PI3K can promote WASP/N-WASP activation in vivo via regulation of small Rho GTPase activity.

Epidermal growth factor (EGF) receptor (EGFR) signalling is strongly linked to breast cancer metastasis (Kim and Muller, 1999) and has a well defined role in the promotion of cell motility (Wells et al., 1998). Class 1A PI3Ks are key effectors in EGF/EGFR signal transduction (Moghal and Sternberg, 1999). Evidence for an EGF/EGFR signalling pathway for the activation of N-WASP includes the finding that EGFR associates with N-WASP in fibroblasts via an interaction with Grb2 (Miki et al., 1996; She et al., 1997). Furthermore, filopodia production in Cos7 cells is attenuated by an N-WASP mutant that fails to bind actin (Miki and Takenawa, 1998).

Urokinase-type plasminogen activator (uPA) is a serine protease that binds to the glycosyl phosphatidylinositol (GPI)-anchored uPA receptor (uPAR). uPA/uPAR expression is strongly correlated with the metastatic potential of breast carcinomas (Andreasen et al., 1997; Foekens et al., 2000) and represents a viable target for anti-tumour therapy (Schmitt et al., 2000). uPA bound to uPAR exhibits enhanced proteolytic activity and directly activates plasminogen, matrix metalloproteinases and growth factors at the cell surface, which gives rise to enhanced extracellular matrix degradation, cell migration and proliferation (Andreasen et al., 1997; Preissner et al., 2000). Ligation of uPA with uPAR can activate cellular responses that are independent of any pericellular proteolytic activity. Non-proteolytic uPA stimulates chemotaxis/migration through the activation of Src-type kinase p56/p59hck, protein kinase C and extracellular signal-regulated kinase (Busso et al., 1994; Chiaradonna et al., 1999; Degryse et al., 1999; Degryse et al., 2001; Fibbi et al., 1998; Nguyen et al., 1999; Nguyen et al., 2000; Resnati et al., 1996). uPAR lacks a transmembrane domain and must associate with transmembrane adaptor protein(s) to activate intracellular signalling molecules. Direct interaction of uPAR with integrins located in the plasma membrane stimulates signal transduction and regulates molecular changes in integrin-containing complexes (Bohuslav et al., 1995; Carriero et al., 1999; Ossowski and Aguirre-Ghiso, 2000; Priessner et al., 2000; Simon et al., 2000; Sitrin et al., 1996; Wei et al., 1996; Xue et al., 1997; Yebra et al., 1999). uPAR overexpression in fibroblast cell lines and its direct binding to vitronectin induces membrane protrusions and increased migratory speed through activation of Rac1 (Kjoller and Hall, 2001). uPAR ligation with uPA promoted cytoskeletal changes and chemotaxis in vascular smooth muscle cells through a pertussis-toxin-sensitive mechanism and a pathway involving Tyk2 and PI3K (Degryse et al., 1999; Degryse et al., 2001; Kusch et al., 2000).

We considered whether PI3K was required for chemotaxis and signalling to Rho GTPases and N-WASP in response to uPAR and EGFR ligation. PI3K was essential for Cdc42, Rac1 and N-WASP activation and chemotaxis induced by EGF but was not required for similar responses induced by uPA. A β_1-integrin-dependent mechanism for the activation of N-WASP by uPA that supports PI3K-independent chemotaxis is also proposed.

Materials and Methods

Reagents and antibodies

Wild-type uPA and mut C uPA were prepared and assayed for proteolytic activity as previously described (Hamelin et al., 1993). Recombinant human epidermal growth factor were from R&D (UK). LY 294002 was from Calbiochem (UK). Growth-factor-depleted Matrigel® was from Stratech Ltd (Luton, UK). Affinity-purified rabbit anti-rat N-WASP polyclonal antibody was a gift from Marc Kirschner (Harvard Medical School, Boston, USA) (Rohatgi et al., 1999). Mouse anti-human β_1-integrin subunit monoclonal antibodies used for immunoprecipitation, immunocytochemistry (clone 8E3) and neutralisation (clone 3S3) and mouse anti-human β_3-integrin subunit monoclonal antibody were from Serotec (UK). Mouse anti-human vinculin was from Sigma (Poole, UK). Mouse anti-human β_1-integrin subunit, rabbit anti-human Akt, rabbit anti-human phospho-Akt and mouse monoclonal anti-human Rac1 (clone 23A8) antibodies used for western blotting were from Upstate Biotechnology (UK). Anti-Cdc42 used for western blotting was from Santa Cruz (UK). Alexa-568-conjugated phalloidin, Alexa-488-conjugated rabbit anti-mouse antibody and Alexa-488-conjugated goat anti-rabbit antibody were from Molecular Probes (UK). Glutathione agarose beads, HRP-conjugated anti-mouse and anti-rabbit antibodies were from Amersham (UK). GST-PAK-CRIB expressing bacteria were a gift from Anne Ridley (Ludwig Institute, University College London, UK). All other chemicals were from Sigma (Poole, UK) or BDH (UK).

Cell culture

MDA MB 231 cells, a highly invasive and oestrogen-receptor-negative human breast carcinoma cell line of epithelial origin were from ECACC. Unless otherwise stated, media and supplements were from Gibco BRL (UK). Cells were grown and passaged in DMEM containing 10% v/v heat inactivated foetal calf serum (FCS) (Biopharm, UK), penicillin/streptomycin (100 IU/ml and 100 μg/ml) and 2 mM L-glutamine. Cells were grown at 37°C in T25 tissue culture flasks (Falcon, UK) and maintained in a humid atmosphere of 5% CO_2. Cells were subcultured when 70-80% confluent by washing twice in Versene (0.2% v/v EDTA solution), incubated for 1-2 minutes in non-enzymatic cell disassociation buffer, resuspended in growth medium and seeded into fresh T25 flasks at a ratio of 1:5. Cells were used from passages 2-15 after recovery of stocks from liquid nitrogen. For culture of cells on Matrigel®, coverslips or culture dishes were thinly coated with Matrigel® (0.5 $\mu g/cm^2$) diluted in DMEM for 1 hour at room temperature and washed twice with PBS before seeding. Cells were allowed to adhere for 4 hours in a 37°C and 5% CO_2 humidified incubator. To obtain serum-starved cultures, cells were washed twice with phosphate-buffered saline (PBS) and maintained for 24 hours in serum-starvation medium (DMEM as above containing 0.1% FCS).

Immunocytochemistry

Cells seeded on Matrigel®-coated coverslips (13 mm diameter) at a density of 2.5×10^3 cells/coverslip were serum starved for 24 hours. Cells were fixed for 10 minutes in 4% w/v paraformaldehyde/3% w/v sucrose in PBS, warmed to 37°C, washed three times with PBS, permeabilised with 0.5% v/v Triton X-100 in PBS for 5 minutes and blocked with 2% v/v bovine serum albumin (BSA) in PBS for 20 minutes at room temperature. Actin filaments in cells were localised by incubation with 0.1 μg/ml Alexa-568-conjugated phalloidin for 1 hour at room temperature. β_1-integrins, vinculin or N-WASP cells were visualised by incubation with 1/500 dilution of anti-β_1-integrin (clone 8E3), 1/200 dilution of anti-vinculin or 1/200 dilution of anti N-WASP in PBS containing 1% w/v BSA for 1 hour at room temperature, followed by incubation with 1/200 Alexa-488-conjugated anti-mouse/rabbit IgG for 45 minutes. Coverslips were mounted on slides using 10% w/v Mowiol in PBS containing 0.1% w/v P-phenylenediamine and visualised using a Leica TCS NT confocal laser scanning head attached to a Leica DM RXA optical microscope (Leica Inc., St. Gallen, Switzerland). Leica TCS scanning software was used to transpose four sequential images from four

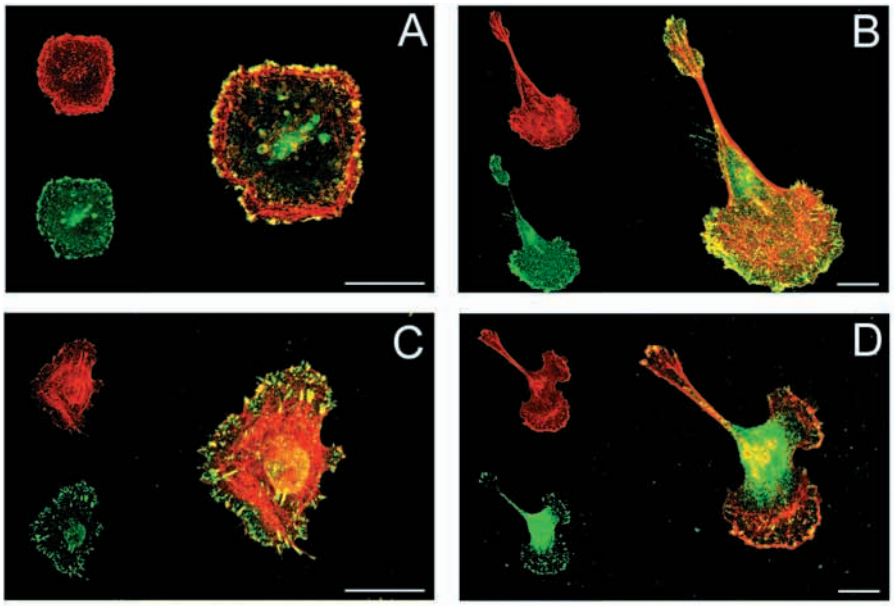

Fig. 1. uPA induces cell polarisation, spreading and redistribution of focal adhesion complexes containing β_1-integrins and vinculin. (A,C) Unstimulated cells. (B,D) Cells stimulated with 10 nM mut C uPA for 30 minutes. (A-D) Alexa-568-conjugated phalloidin; (A,B) Anti-β_1-integrins labelled with Alexa-488-conjugated secondary antibody; (C,D) Anti-vinculin labelled with Alexa-488-conjugated secondary antibody. Bar, 10 μm. Images are representative of three experiments.

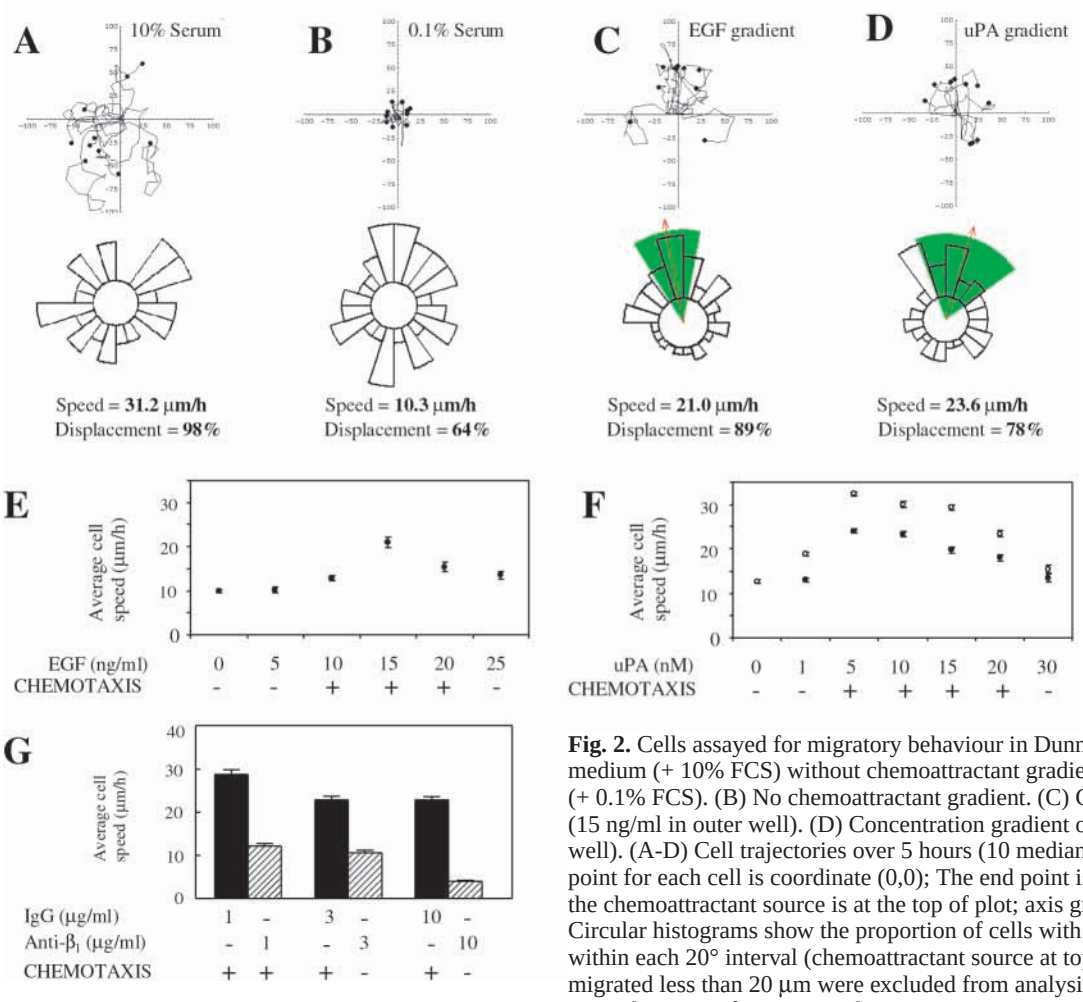

Fig. 2. Cells assayed for migratory behaviour in Dunn chambers. (A) Growth medium (+ 10% FCS) without chemoattractant gradient. (B-D) Starvation medium (+ 0.1% FCS). (B) No chemoattractant gradient. (C) Concentration gradient of EGF (15 ng/ml in outer well). (D) Concentration gradient of mut C uPA (10 nM in outer well). (A-D) Cell trajectories over 5 hours (10 median cell trajectories). The start point for each cell is coordinate (0,0); The end point is marked by a closed circle; the chemoattractant source is at the top of plot; axis graduations, distance (μm). Circular histograms show the proportion of cells with migratory direction lying within each 20° interval (chemoattractant source at top of histogram). Cells that migrated less than 20 μm were excluded from analysis. The red arrow represents the mean direction of migration; the green segment represents the 95% confidence interval determined by the Rayleigh test. Displacement shows the percentage of cells that migrate further than 20 μm. Concentration-dependent response for (E) EGF, (F) wt uPA (open circles) and mut C uPA (closed circles). (G) Effect of β_1-integrin neutralising antibody and mouse IgG antibody on chemotaxis stimulated by 10 nM mut C. More than 40 cells pooled from three to six experiments included in analyses.

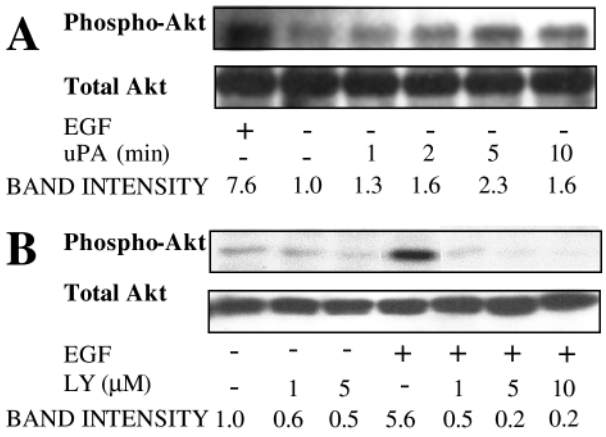

Fig. 3. Total Akt and phosphorylated Akt in whole cell lysates determined by SDS PAGE on 10% gels and immunoblotting. Cells were stimulated with 10 ng/ml EGF for 10 minutes or 10 nM mut C uPA. (A) uPA activated Akt phosphorylation. (B) Inhibition of EGF-stimulated Akt phosphorylation by 1-10 μM LY 294002 (pre-treatment 1 hour). Relative band intensities represent the ratio of phospho-Akt to total Akt (band intensity in unstimulated cells, 1.0). The results are representative of three experiments.

separate optical sections taken at equal distances from the bottom to the top of the cell. The same software was used to merge confocal images. Cytoskeletal features were quantified in fields of view blindly selected at random.

Chemotaxis assays

Chemotaxis was assessed by direct observation and recording of cell behaviour in stable concentration gradients of wild-type or mut C uPA or EGF using the Dunn chamber chemotaxis chamber (Weber Scientific International Ltd., Teddington, UK). This apparatus permits speed, direction of migration and displacement of individual cells to be measured in relation to the direction of a gradient (Zicha et al., 1991). Details of the construction and calibration of Dunn chambers is found elsewhere (Allen et al., 1998; Webb et al., 1996; Zicha et al., 1991). The chamber was filled with serum starvation medium (with or without inhibitory agents) and a Matrigel®-coated coverslip (18 mm×18 mm) with cells seeded at a density of 5×10^3 cells per coverslip was inverted and fixed onto the chamber. Serum starvation medium containing wild-type or mut C uPA or EGF (with or without inhibitory agents) was placed into the outer well of the chamber. Chambers were maintained at 37°C and frame grabbing time-lapse recording of cells located on the bridge of the Dunn chamber was started within 15 minutes of assembly. Images of cells were digitally recorded at a time-lapse interval of 10 minutes for 5 hours using the Kinetic Imaging AQM System (Kinetic Imaging, Liverpool, UK). Cells were tracked and analysed as described previously (Allen et al., 1998; Vanhaesebroeck et al., 1999). Scatter plots of cell trajectories for the 5 hour duration of each assay were constructed on x,y axis plots, where the start point is coordinate (0,0) and the end point of each cell marked with a closed circle. 10 median cell trajectories from the total cell population were selected using a customised Mathematica™ notebook (Graham A. Dunn, King's College London, London, UK). Circular histograms were constructed using Mathematica™ 3.0 for Windows 95 (Wolfram Research Inc., Champaign, IL, USA) as described previously (Allen et al., 1998; Vanhaesebroeck et al., 1999). A virtual horizon of 20 μm was applied to MDA MB 231 cells owing to their larger size. The Rayleigh test for unimodal clustering of directions (Mardia, 1972) was used to assess whether the cell population pooled from several separate experiments displayed directionality in the chemotactic gradient. Average speed and cell displacement were calculated. Displacement equals the % cells that migrate further than 20 μm (Jones et al., 2000).

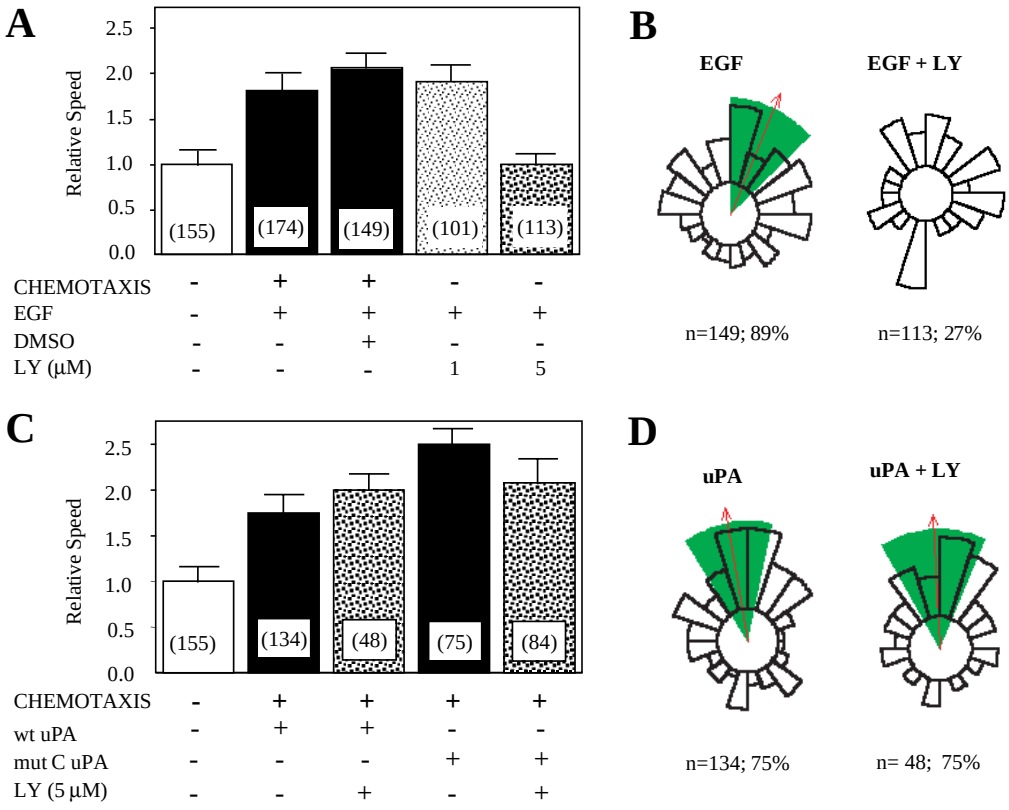

Fig. 4. PI3K-independent chemotaxis stimulated by uPA in Dunn chamber chemotaxis assay. (A,B) EGF (15 ng/ml). (C,D) 15 nM mut C uPA. (A,C) Relative cell speeds (basal cell speed=1.0). Positive/negative chemotactic response (+/–) (total number of cells). (B,D) Directionality/displacement of cells stimulated by EGF and uPA±5 μM LY 294002. Mean direction of cell migration (red arrow)/95% confidence interval (green wedge) determined by Rayleigh test. *n*=total number of cells assayed in three to six experiments.%=proportion of cells that migrate further than 20 μm.

Total cell lysates

Cells were washed in ice-cold PBS before addition of ice-cold RIPA buffer (50 mM Tris-HCl pH 7.5,

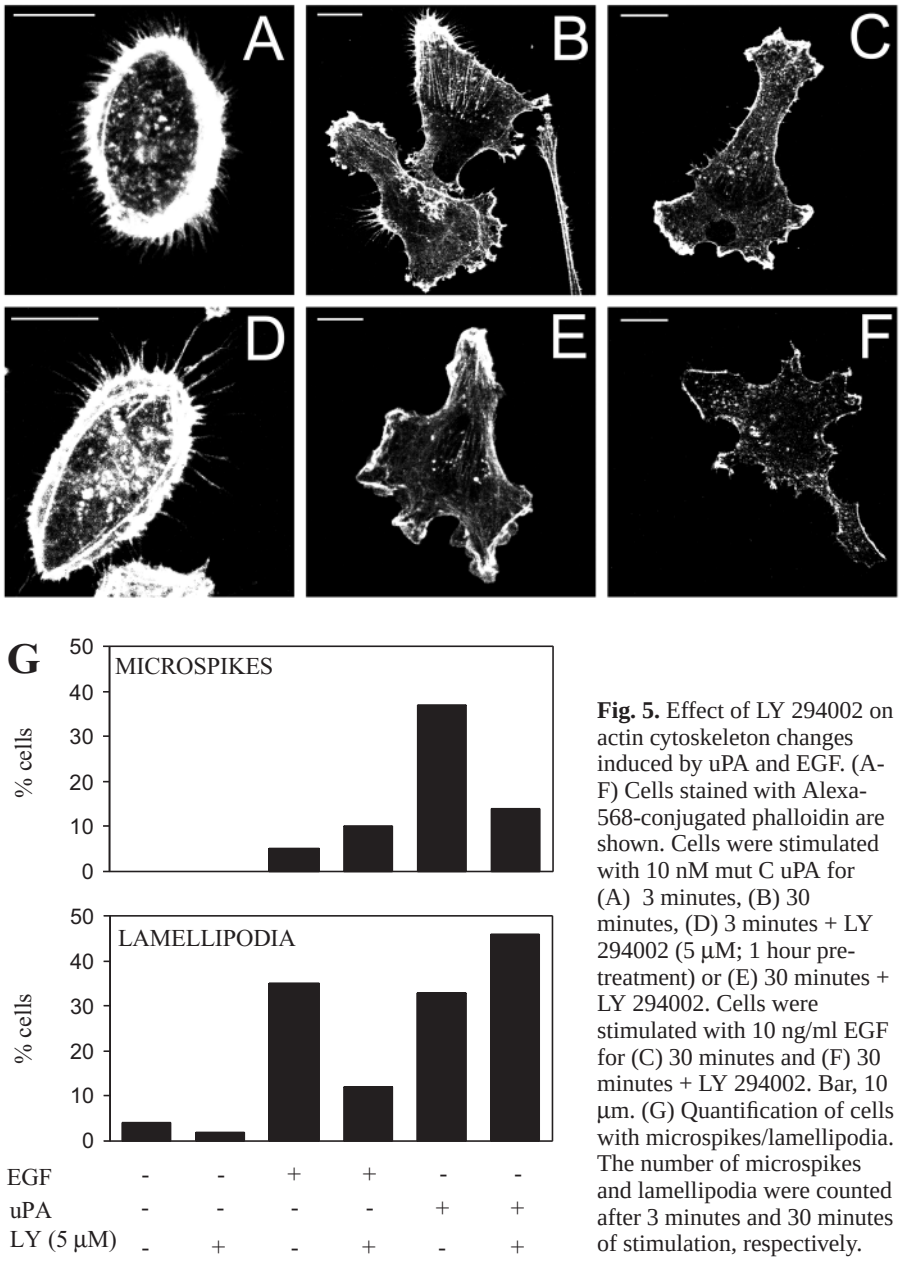

Fig. 5. Effect of LY 294002 on actin cytoskeleton changes induced by uPA and EGF. (A-F) Cells stained with Alexa-568-conjugated phalloidin are shown. Cells were stimulated with 10 nM mut C uPA for (A) 3 minutes, (B) 30 minutes, (D) 3 minutes + LY 294002 (5 μM; 1 hour pre-treatment) or (E) 30 minutes + LY 294002. Cells were stimulated with 10 ng/ml EGF for (C) 30 minutes and (F) 30 minutes + LY 294002. Bar, 10 μm. (G) Quantification of cells with microspikes/lamellipodia. The number of microspikes and lamellipodia were counted after 3 minutes and 30 minutes of stimulation, respectively.

150 mM NaCl, 1 mM EDTA, 1 mM EGTA, 5 mM sodium molybdate, 1% v/v sodium deoxycholate, 1% v/v Nonidet P-40, 1% Triton X-100, 0.1% SDS) containing 50 mM sodium fluoride, 1 mM sodium orthovanadate, 20 mM sodium phenylphosphate, 1 mM phenylmethylsulfonyl fluoride, 10 μg/ml aprotonin, 5 μg/ml leupeptin and 2 μg/ml pepstatin A. Cells were incubated for 15 minutes at 4°C, scraped and passed through a 25 gauge needle five times before clarifying by centrifugation (16,000 ***g***, 4°C, 10 minutes). Protein content was measured (Bio Rad protein assay kit).

Akt phosphorylation assay

Total cell lysates (15 μg protein per well) were resolved on 10% SDS PAGE gels. Protein was electrotransferred onto polyvinylidinefluoride (PVDF) membranes (Immobilon-P; Millipore, UK). Membranes were incubated in blocking buffer (2% BSA and 0.1% v/v Tween 20 in Tris buffered saline (TBS): 20 mM Tris HCl pH 7.5, 0.5 M NaCl) for 1 hour at room temperature and probed with 1/1000 dilution anti-phospho-Akt or anti-total Akt in blocking buffer at 4°C for 16 hours. Membranes were washed five times for 5 minutes, incubated for 1 hour at room temperature with 1/2000 dilution of HRP-conjugated anti-mouse IgG in blocking buffer, washed five times with TBS containing 0.1% Tween 20. Antibody-reactive proteins were detected using chemiluminescent substrate (ECL Plus; Amersham UK). Equivalent samples of cell lysates were loaded in duplicate on separate gels to allow analysis of both phospho-Akt and total Akt.

Cdc42 and Rac1 activity assay

Cells grown on Matrigel®-coated 60 mm dishes were used at 50% confluence. Cells washed once with ice-cold PBS and 550 μl ice-cold GST-PAK-CRIB assay lysis buffer (50 mM Tris-HCl pH 7.4, 100 mM NaCl, 1 mM $MgCl_2$, 1% v/v Nonidet P-40; 10% v/v glycerol, 10 mM sodium fluoride, 1 mM sodium orthovanadate, 1 mM phenylmethylsulfonyl fluoride, 10 μg/ml aprotonin, 5 μg/ml leupeptin and 2 μg/ml pepstatin A) were added. Cells were scraped and cleared by centrifugation (16,000 ***g***, 4°C, 1 minute). 50 μl of cleared lysate was retained for analysis of total Rac1/Cdc42 by western blotting. 500 μl of cleared lysate was mixed by inversion for 1 hour at 4°C with 25 μl of freshly prepared slurry containing 20 μg GST-PAK-CRIB fusion protein coupled to glutathione-conjugated agarose beads (Amersham, UK). Preparation of beads is described elsewhere (Sander et al., 1998). Beads were pelleted by pulse centrifugation (16,000 ***g***, 4°C, 1 minute), washed three times in GST-PAK-CRIB assay lysis buffer and split in two before a final pulse centrifugation. Duplicate samples of pelleted beads were analysed for Rac1/Cdc42 content. PAK-CRIB precipitated GTP-bound active Rac1/Cdc42, and total Rac1/Cdc42 from corresponding unprecipitated cell lysates were resolved on 12% SDS PAGE gels. Western blotting for Rac1/Cdc42 was carried out as described for Akt phosphorylation assays except the blocking buffer contained 5% non-fat dry milk (Blocker; Bio Rad, UK). 1/2000 dilution of mouse anti-Rac1 monoclonal antibody (clone 23A8) was used with 1/3000 dilution of HRP-conjugated anti-mouse IgG or 1/500 dilution of rabbit anti-Cdc42 polyclonal antibody was used with 1/2000 HRP-conjugated anti-rabbit IgG. The ratio of active Rac1/Cdc42 to total Rac1/Cdc42 was calculated by scanning densitometry of immunoreactive bands (Imaging software, Kinetic Imaging, UK).

Immunoprecipitation

Cells grown on Matrigel®-coated 60 mm dishes were used at 50% confluence. Cells were washed once with ice-cold microtubule stabilisation buffer (0.1 M PIPES HCl pH 6.92, 2 M glycerol, 1 mM EGTA, 1 mM magnesium acetate) and incubated with Triton X-100 lysis buffer (50 mM Tris-HCl pH 7.5, 150 mM NaCl, 1 mM EDTA, 1 mM EGTA, 0.2% Triton X-100; 50 mM sodium fluoride, 1 mM

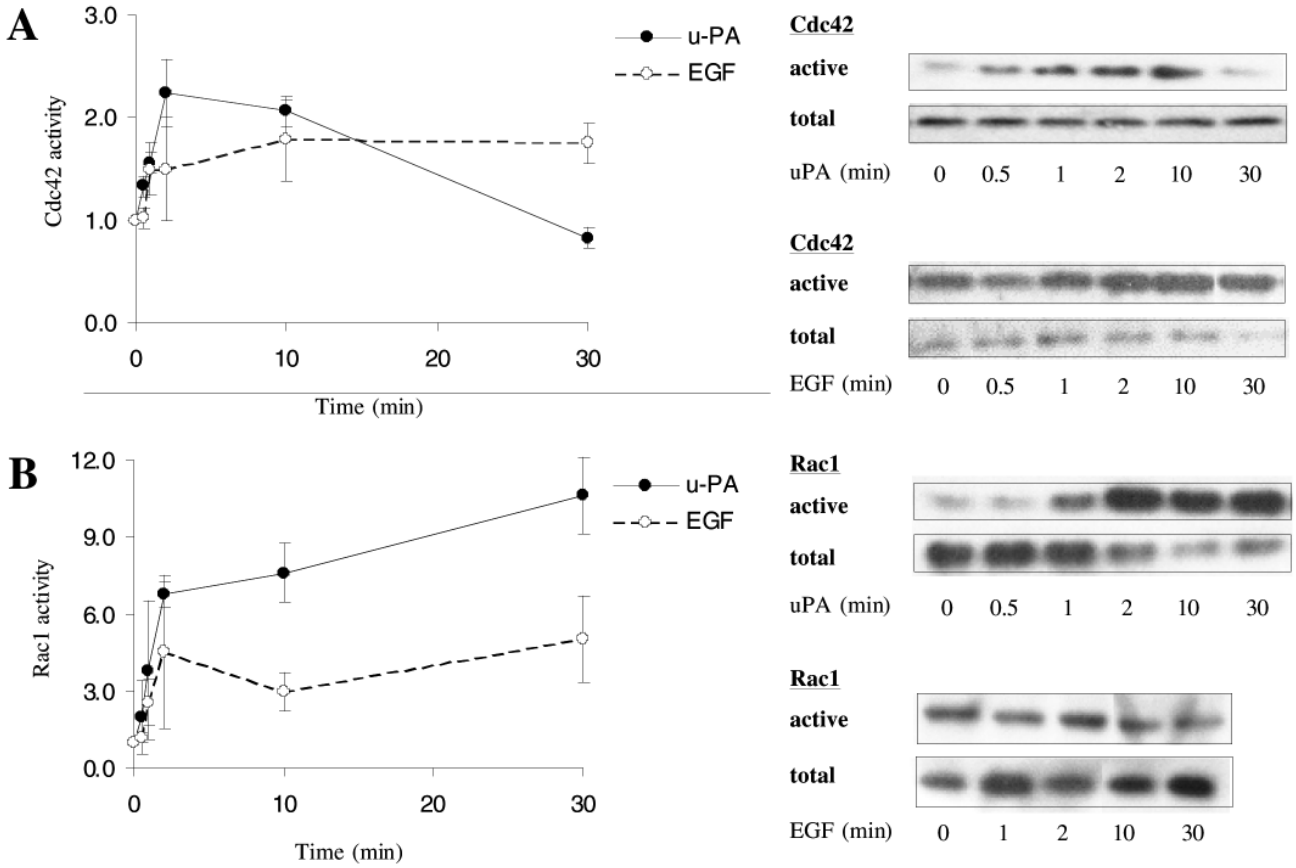

Fig. 6. Cdc42 and Rac1 activation by uPA and EGF. (A,B) Cells were assayed for Cdc42/Rac1 GTPase activation using a PAK-CRIB pull down assay. The levels of total cellular Rac1/Cdc42 and GST-PAK-CRIB that precipitated Cdc42/Rac1 were determined by SDS PAGE on 12% gels and immunoblotting. Temporal activation of (A) Cdc42 and (B) Rac1 by 10 nM uPA and 10 ng/ml EGF are shown. Graphs show ratios of GST-PAK-CRIB bound to total Cdc42/Rac1 (band intensity in unstimulated cells, 1.0). The results represent mean±s.e.m. from three to seven experiments.

sodium orthovanadate, 20 mM sodium phenylphosphate, 1 mM phenylmethylsulfonyl fluoride, 10 μg/ml aprotonin, 5 μg/ml leupeptin and 2 μg/ml pepstatin A) for 15 minutes at 4°C. Lysed cells were scraped and cleared by centrifugation (16,000 ***g***, 4°C, 10 minutes). Lysates with equal protein content (0.5 mg/ml) were mixed by inversion with 25 μl of slurry containing protein A agarose for 30 minutes at 4°C to pre-clear. Beads were pelleted by pulse centrifugation and the supernatant mixed by inversion with 4 μg/ml of antibody (anti-EGFR; anti-β_1-integrin (clone 8E3)) overnight at 4°C. Immunocomplexed proteins were precipitated by adding 25 μl of slurry containing protein A agarose for 1 hour at 4°C followed by pulse centrifugation. Immunocomplexed proteins in protein A agarose bead pellets were resolved on 12% SDS PAGE gels. Western blot analysis was carried out as described for Akt phosphorylation except the blocking buffer contained 5% non-fat dry milk. 1/1000 dilution of mouse β_1-integrin monoclonal antibody (Upstate Biotechnology) was used with 1/2000 dilution of HRP-conjugated anti-mouse IgG. 1/1000 dilution of rabbit anti-EGFR or 1/4000 dilution of rabbit anti-N-WASP polyclonal antibodies was used with 1/2000 HRP-conjugated anti-rabbit IgG.

Cytoskeletal N-WASP assay

The method of Wei et al. was used to separate the cytosolic and cytoskeletal fractions of MDA MB 231 cells (Wei et al., 1996). Cells grown on Matrigel®-coated 60 mm dishes were used at 50% confluence. Cells were washed with ice-cold microtubule stabilisation buffer, incubated in 500 μl Triton X-100 lysis buffer (as used for immunoprecipitation) at 4°C for 15 minutes, scraped and cleared by centrifugation (16,000 ***g***, 4°C, 10 minutes). The supernatant was retained for analysis of the N-WASP content of Triton X-100 soluble (cytosolic) fraction. Pelleted Triton X-100 insoluble material was washed three times in 1 ml Triton X-100 lysis buffer containing 0.1% v/v Triton X-100. Pelleted material was resuspended in 250 μl RIPA buffer (as used for total cell lysates) by passing through a 25-gauge needle five times, incubated at 4°C for 15 minutes, cleared by centrifugation (16,000 ***g***, 4°C, 10 minutes) and analysed for N-WASP content of Triton X-100 insoluble (cytoskeletal) fraction. Lysates of cytosolic and cytoskeletal fractions (15 μg per well) were resolved on 10% SDS PAGE gels and analysed for N-WASP by western blot.

Results

uPA alters cell morphology and focal adhesion complex organisation

As demonstrated in other types of cancer cell (Xue et al., 1997; Yebra et al., 1999), we showed that uPAR and β_1-integrins can be coimmunopreciptated from the MDA MB 231 breast cancer cell line, which expresses high endogenous levels of uPAR. We also observed a substantially increased association of uPAR and β_1-integrins in uPA-stimulated cells (data not shown). It has also previously been shown that proteins associated with

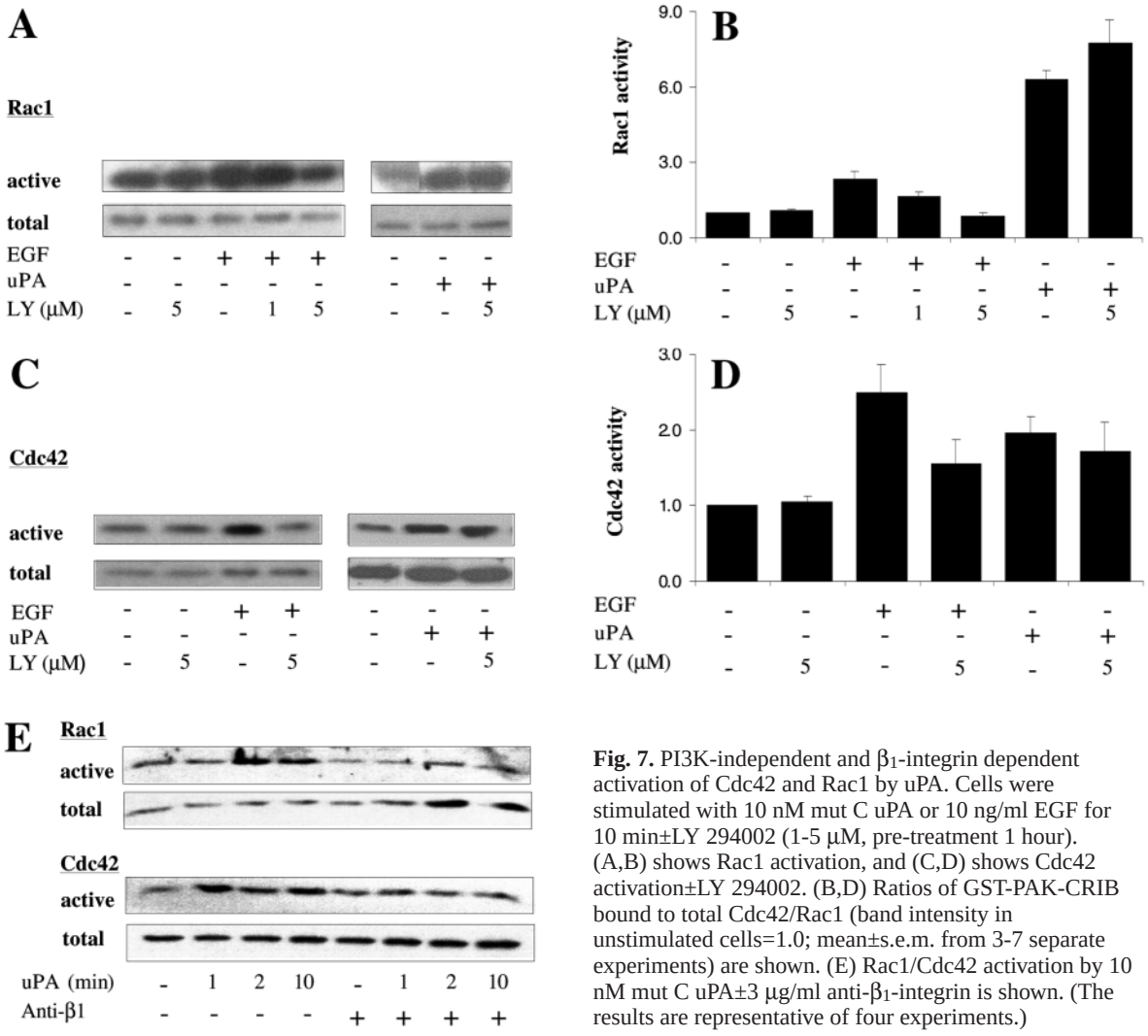

Fig. 7. PI3K-independent and β_1-integrin dependent activation of Cdc42 and Rac1 by uPA. Cells were stimulated with 10 nM mut C uPA or 10 ng/ml EGF for 10 min±LY 294002 (1-5 μM, pre-treatment 1 hour). (A,B) shows Rac1 activation, and (C,D) shows Cdc42 activation±LY 294002. (B,D) Ratios of GST-PAK-CRIB bound to total Cdc42/Rac1 (band intensity in unstimulated cells=1.0; mean±s.e.m. from 3-7 separate experiments) are shown. (E) Rac1/Cdc42 activation by 10 nM mut C uPA±3 μg/ml anti-β_1-integrin is shown. (The results are representative of four experiments.)

linkage of integrins to the cytoskeleton, such as vinculin, colocalise with uPAR (Hebert and Baker, 1988). We determined that uPA promoted changes in the actin cytoskeleton and β_1-integrin subunit/vinculin containing complexes in MDA MB 231 cells. To ensure that the effects of uPA were non-proteolytic, we compared the effects of enzymatically active and inactive uPA. Proteins were made from constructs encoding single chain uPA wild-type recombinant uPA (wt-uPA) and recombinant uPA targeted by site-directed mutagenesis in its catalytic domain (mut C uPA) (Hamelin et al., 1993). Recombinant uPA proteins were analysed for their amidolytic and fibrinolytic activities and their ability to bind uPAR (Hamelin et al., 1993) before being used to stimulate cells. Throughout this study we found that wild-type and mut C uPA induced similar effects on MDA MB 231 cells, confirming the involvement of a non-proteolytic intracellular signalling mechanism.

Cells maintained in growth medium (DMEM + 10% FCS) exhibited a variety of morphological structures consistent with a motile phenotype, such as polarisation, abundant membrane ruffles, lamellipodia and protrusions (data not shown). For this reason the effect of uPA on the morphology of growing cells could not be clearly assessed. Under conditions of serum starvation (DMEM + 0.1% FCS for 24 hours), the majority of cells were not polarised, having very few lamellipodial protrusions and membrane ruffles; 60% of cells had peripheral actin rings (Fig. 1A) and 50% of cells had stress fibres/actin cables (Fig. 1C). Abundant membrane ruffles, lamellipodial protrusions and polarisation were seen in uPA-stimulated cells after 30 minutes (Fig. 1B,D). uPA stimulation also caused rearrangement and redistribution of focal adhesion complexes containing vinculin and β_1-integrins. In unstimulated cells, small punctate β_1-integrin rich complexes were concentrated around the cell periphery and sparsely dotted throughout the cell body (Fig. 1A). In uPA-stimulated cells these small focal adhesions disappeared and were replaced by much larger structures containing β_1-integrins that localised to the leading edge and rear of the cell (Fig. 1B). The large vinculin rich focal adhesions,which colocalised to the ends of actin stress fibres in unstimulated cells, (Fig. 1C) were absent in uPA-stimulated cells; instead smaller punctate and more diffuse vinculin-containing structures were seen (Fig. 1D). Similar turnover of vinculin and β_1-integrin subunit containing structures has been observed in various migratory cells (Adams, 2001). For this reason we decided to assess the effect of uPA on the migratory response of MDA MB 231 cells.

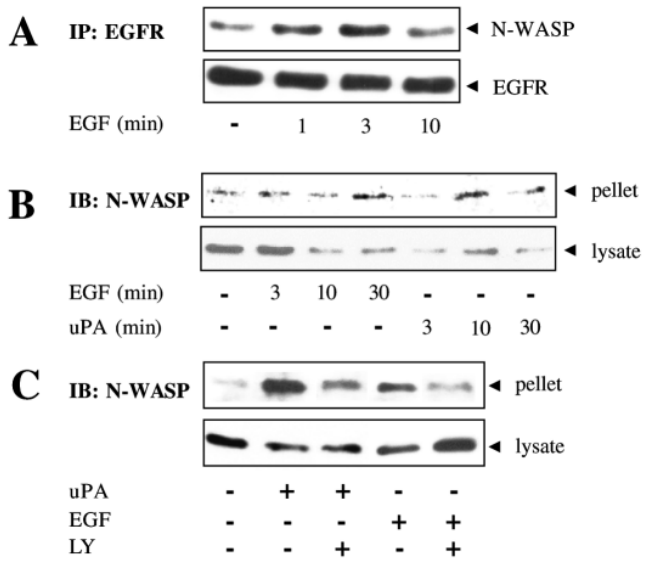

Fig. 8. uPA and EGF activate N-WASP with divergent requirement for PI3K. (A) Cells were stimulated with 10 ng/ml EGF for 1-10 minutes. EGFR immunoprecipitates were separated on 10% gels and immunoblotted for N-WASP. (B,C) shows N-WASP in Triton X100 soluble cell lysates (cytosolic fraction) and Triton X100 insoluble cell pellets (cytoskeletal fraction). (B) Cells stimulated with 10 ng/ml EGF or 10 nM uPA for 1-30 minutes are shown. (C) Cells stimulated for 10 minutes with 10 nM mut C uPA or 10 ng/ml EGF±LY 294002 are shown (5 μM; pre-treatment 1 hour). The results are representative of three to six experiments.

uPA and EGF induce chemotaxis that is dependent on β_1-integrins

As reported above, MDA MB 231 cells maintained in 10% FCS on a Matrigel® substratum polarised in various orientations. Cells assayed in Dunn chambers under similar conditions displayed fast (>30 μm/h) random migration and maximum levels of displacement, with nearly 100% cells migrating beyond a 20 μm horizon within the 5 hour duration of the assay (Fig. 2A). In contrast, cells maintained in DMEM + 0.1% FCS for 24 hours exhibited markedly decreased migratory speeds and displacement (Fig. 2B). We compared the chemotactic response of MDA MB 231 cells to uPA with that to EGF, a known chemotactic factor in fibroblasts and breast cancer cells (Wells et al., 1998). MDA MB 231 cells express high levels of EGFR, and we confirmed that EGF increased phosphorylation of EGFR in this cell type (C. Sawyer, unpublished). Serum-starved cells assayed in isotropic concentrations of EGF, wild-type uPA or mut C uPA displayed increased speed with random directionality (data not shown), similar to cells maintained in growth medium. When serum-starved cells were placed in linear gradients of EGF (Fig. 2C,E), mut C or wild type uPA (Fig. 2DF), speed and displacement were increased. Moreover, cells displayed unimodal upgradient polarisation and positive chemotaxis towards the source of EGF or uPA. The concentration of chemoattractant used was found to be critical for the migratory and chemotactic response. Increased migratory speed and chemotaxis was only observed at 10-25 ng/ml EGF (Fig. 2E) and 5-25 nM uPA (Fig. 2F). Optimal chemotaxis occurred in gradients generated with 15 ng/ml EGF or 5 nM uPA in the outer well. Mut C uPA stimulated higher migratory speeds than wt uPA over the same concentration range (Fig. 2F).

The chemotactic responses of cells to EGF and uPA required β_1-integrins. Incubation of cells with anti-β_1-integrin subunit neutralising antibody inhibited increases in cell speed and chemotaxis stimulated by both EGF (data not shown) and uPA (Fig. 2G), whereas anti-β_3-integrin subunit antibody had no effect on the same parameters (data not shown).

uPA stimulates chemotaxis in a PI3K-independent manner

Class 1A PI3Ks have roles in signalling to the actin cytoskeleton and driving the chemotactic response (Arrieumerlou et al., 1998; Hill et al., 2000; Hirsch et al., 2000; Jones, 2000; Li et al., 2000; Reif et al., 1996; Vanhaesebroeck et al., 1999). It has recently been suggested that uPA can signal through the interaction of Tyk2 and PI3K to promote cytoskeletal changes and migration in vascular smooth muscle cells (Kusch et al., 2000). Therefore, we considered whether uPA could signal through PI3K in MDA MB 231 cells. In our studies we used EGF stimulation as a positive control for PI3K-dependent signalling. Immunoblot analysis of whole cell lysates indicated that both EGF- and mut C uPA-stimulation increased the phosphorylation of Akt (Fig. 3A), which is a well defined downstream effector of PI3K (Vanhaesebroeck and Waterfield, 1999). In addition, LY 294002 totally negated EGF and uPA induced Akt phosphorylation (Fig. 3B) at concentrations (1-10 μM) that exclusively inhibit class 1A PI3Ks (Vanhaesebroeck and Waterfield, 1999). LY 294002 vehicle alone (0.005-0.05% v/v DMSO) had no effect on Akt phosphorylation stimulated by either EGF or mut C uPA (data not shown). These findings confirm that both EGF and uPA are capable of signalling through PI3K.

We next considered whether signalling through PI3K was required for the chemotactic and/or migratory response of MDA MB 231 cells in a gradient of uPA. EGF gradients were used as a comparative control. Cells were analysed in EGF and uPA gradients using LY 294002 at the same concentrations that inhibited Akt phosphorylation. Observation of MDA MB 231 cells using time-lapse recording indicated that LY 294002 did not affect the random migration of serum starved cells at concentrations below 20 μM. The chemotactic response of cells in an EGF gradient was sensitive to inhibition by 1 μM LY 294002, with no effect on random cell movement and speed (Fig. 4A,B). Addition of 5 μM LY 294002 completely attenuated the increase in speed and chemotaxis stimulated by EGF. In contrast, the chemotaxis of cells in linear gradients of wild-type uPA or mut C uPA was not affected by the presence of LY 294002 (1-10 μM) (Fig. 4C,D). In conclusion our data strongly suggested that uPA does not require PI3K to promote chemotactic and migratory responses in MDA MB 231 cells despite being activated (as judged by increased Akt phosphorylation).

The majority of cytoskeletal rearrangements induced by uPA are PI3K independent

The effect of inhibition of PI3K on actin cytoskeleton rearrangements stimulated by uPA and EGF was investigated.

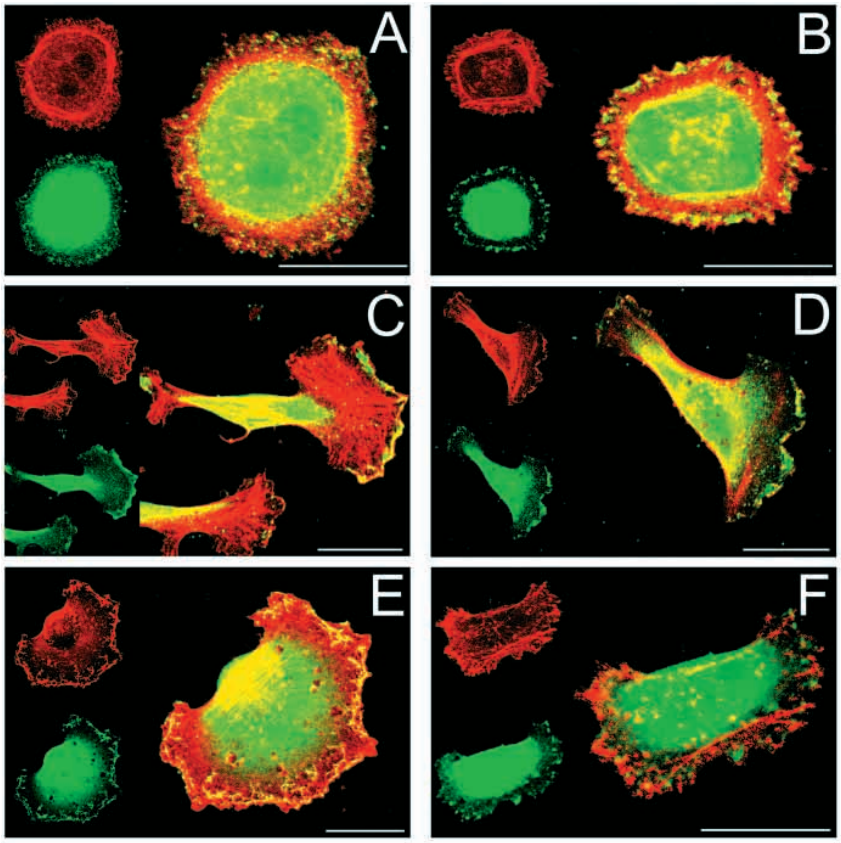

Fig. 9. uPA and EGF stimulate N-WASP colocalisation to F-actin with divergent requirement for PI3K activity**.** (A-F) shows cell staining with Alexa-568-conjugated phalloidin and anti-N-WASP labelled with Alexa-488-conjugated secondary antibody. (A,B) shows unstimulated cells in the (A) absence and (B) presence of LY 294002 for 30 minutes (5 μM; pre-treatment 1 hour). (C,D) The result of a 30 minute stimulation with 10 nM mut C uPA in the (C) absence and (D) presence of LY 294002 is shown. (E,F) 30 minutes stimulation with 10 ng/ml EGF in (E) absence and (F) presence of LY 294002 is shown. Images are representative of three experiments. Bar, 10 μm.

The most notable difference in cytoskeletal changes induced by the two chemoattractants was the strong and rapid induction of microspike extensions by uPA but not EGF. Microspike extensions were not observed in unstimulated cells; 37% of cells produced microspikes after 3 minutes of uPA stimulation (Fig. 5A,G), and 5% of cells produced microspikes after 3 minutes EGF stimulation (Fig. 5G). Microspikes formed in response to uPA with and without addition of LY 294002 were similar in length and structure (Fig. 5A,D). However, LY 294002 decreased the number of cells that formed microspikes in response to uPA by ~60% (Fig. 5G). In contrast there was no inhibitory effect of LY 294002 on uPA-induced membrane ruffles, lamellipodia or cell polarisation (Fig. 5B,E). In fact the number of cells with lamellipodial extensions stimulated by uPA was increased by ~40% in the presence of LY 294002. In contrast, LY 294002 almost totally negated membrane ruffles, lamellipodia and polarisation stimulated by EGF (Fig. 5C,F). Most notably, the number of EGF-stimulated cells that formed lamellipodia was decreased by ~65% in the presence of LY 294002 (Fig. 5G). In the presence of LY 294002 there was a modest increase in the proportion of EGF-stimulated cells that produced microspikes (an increase from 5% to 10% of total cell population) (Fig. 5G). However, it should be noted that the microspikes stimulated by EGF were not a major morphological feature of this small fraction of cells, as was the case in uPA stimulated cells.

Cdc42 and Rac1 activation by uPA requires β1-integrins but not PI3K

The cytoskeletal changes and migratory responses induced by uPA in MDA MB 231 cells were similar to those induced by active small Rho GTPase proteins in macrophages and fibroblasts. That is active GTP-bound Cdc42 induces microspike formation and cell polarisation, and active GTP-bound Rac1 induces membrane ruffles, lamellipodia formation and sustained migration (Allen et al., 1997; Allen et al., 1998; Kozma et al., 1995; Ridley et al., 1992).

To investigate whether the differences in cytoskeletal structures induced by uPA and EGF pertained to differences in Cdc42 and Rac1 activation, the levels of GTP-bound Cdc42 and Rac1 were determined. Active Cdc42 and Rac1 were precipitated from lysates of cells treated with EGF or mut C uPA using the Cdc42/Rac1-binding domain of p21-activated kinase (PAK) fused to GST (Sander et al., 1998). First, we determined whether the same concentrations of uPA and EGF that stimulated chemotaxis also activated Rac1 and Cdc42. 10 nM mut C uPA and 10 ng/ml EGF stimulated maximal levels of Rac1 and Cdc42 activation (data not shown), which correlated with the stimulation of chemotaxis and increased migratory speed (Fig. 2). uPA stimulated a transient but substantial increase in active Cdc42 without affecting total cellular Cdc42 (Fig. 6A). Maximum Cdc42 activation occurred after 2 minutes of stimulation, and basal levels were restored by 30 minutes. In contrast, the increase in Cdc42 activation stimulated by EGF was sustained, albeit at a modest level, for at least 30 minutes. Both uPA and EGF activated Rac1 within 2 minutes, and this level of activation was maintained for at least 30 minutes (Fig. 6B).

We next determined whether activation of Rac1 and Cdc42 by EGF and uPA occurred downstream of β_1-integrins and PI3K. LY 294002 inhibited activation of Rac1 and Cdc42 by EGF at concentrations that blocked chemotaxis (Fig. 7A-D). In contrast, LY 294002 had no effect on Rac1 and Cdc42 activation stimulated by uPA (Fig. 7A-D). The requirement of β_1-integrins for chemotaxis in response to EGF and uPA correlated with their involvement in EGF and uPA-induced activation of small Rho GTPases. The same concentrations of anti-β_1-integrin neutralising antibody that inhibited chemotaxis (Fig. 2G) also inhibited Rac1 and Cdc42 activation in response to EGF (data not shown) and uPA (Fig. 7E). Irrelevant mouse IgG did not effect Rac1/Cdc42 activation in response to EGF-uPA (data not shown). This confirms that signalling from uPA-uPAR and EGF-EGFR to the small Rho GTPases requires fully

functional β_1-integrins but has divergent requirement for PI3K activity.

Divergent requirement of PI3K for N-WASP activation by uPA and EGF occurs through a mechanism involving β_1-integrins

The existence of an EGFR/PI3K/N-WASP pathway in MDA MB 231 cells was supported by several findings. (a) N-WASP was detected in EGFR immunoprecipitates and this association was increased upon EGF stimulation (Fig. 8A). (b) N-WASP content increased in the cytoskeletal fraction and decreased in the cytosolic fraction after 10-30 minutes stimulation with EGF (Fig. 8B), an effect that was totally inhibited by LY 294002 (Fig. 8C). (c) N-WASP colocalised with F-actin rich membrane ruffles upon EGF stimulation (Fig. 9E), an effect that was totally inhibited by LY 294002 (Fig. 9F). LY 294002 alone had no effect on N-WASP localisation to F-actin in unstimulated cells (Fig. 9A,B). These findings are in accordance with previous reports of EGFR signalling to N-WASP and induction of actin cytoskeletal rearrangements (Miki et al., 1996; Miki et al., 1998; She et al., 1997) and provide support to a regulatory role for PI3K in N-WASP activation downstream of EGFR.

The dramatic induction of microspikes suggested activation of N-WASP by uPA. N-WASP content increased in the cytoskeletal fraction and decreased in the cytosolic fraction of uPA-stimulated cells (Fig. 8B). The translocation of N-WASP stimulated by uPA occurred after stimulation for 3 minutes (compared with 10 minutes after EGF stimulation) and lasted for at least 30 minutes. Translocation of N-WASP in response to EGF and uPA also differed in sensitivity to LY 294002; the response induced by EGF was totally inhibited whereas that induced by uPA was partially inhibited by the PI3K inhibitor (Fig. 8C). This partial inhibitory effect may explain the decreased number of cells producing microspikes in response to uPA in the presence of LY 294002 (Fig. 5G). Although we could not visualise N-WASP within, or at the base of, uPA-induced microspikes by immunofluorescent staining (data not shown), it colocalised with F-actin at the leading edge of uPA-stimulated cells (Fig. 9C), and this localisation was not affected by PI3K inhibition (Fig. 9D). Taken together these data suggest that both PI3K-dependent and independent activation of N-WASP occurs upon uPAR ligation with uPA.

How does uPAR ligation with uPA induce the rapid activation of N-WASP? We predicted that β_1-integrins, which associate with uPAR upon ligation with uPA, are involved in uPAR signalling to N-WASP. β_1-integrins were required for chemotaxis and Rho GTPase activation by EGF and uPA (Fig. 2G; Fig. 7E), and similar F-actin structures were colocalised with β_1-integrins and N-WASP in unstimulated and stimulated cells (Fig. 1B; Fig. 9C). We analysed β_1-integrin subunit immunoprecipitates for N-WASP content and found the two proteins were associated in unstimulated cells (Fig. 10A). This association was almost totally disrupted in cells stimulated with uPA for 1-3 minutes and was returned to basal levels at 30 minutes (Fig. 10A). The disassociation of β_1-integrin and N-WASP stimulated by uPA also occurred in the presence of LY 294002 (Fig. 10A). In contrast, EGF stimulated partial and latent (after 10 minutes stimulation) disassociation of β_1-integrin-N-WASP, which was totally inhibited by LY 294002 (Fig. 10B).

Discussion

Expression levels of uPA and its receptor uPAR, as well as of EGF and its receptor EGFR, in breast cancer are highly correlated with the incidence of metastasis and poor clinical prognosis (Andreasen et al., 1997; Foekens et al., 2000; Kim and Muller, 1999). Characteristics of the MDA MB 231 breast carcinoma cell line include its highly motile and invasive behaviour and abundant expression of endogenous uPAR and EGFR. Our studies using this cell line in culture have revealed that common chemotactic and cytoskeletal signalling pathways are activated downstream of uPAR and EGFR, but the two receptors were found to be divergent in their requirement for functional PI3K activity.

The stimulatory effects of uPA in MDA MB 231 cells were independent of the proteolytic activity of uPA since both fully proteolytically active wild-type uPA and proteolytically inactive mut C uPA induced similar responses. The only observable difference between the two forms of uPA was that a faster migratory speed was induced by mut C uPA, an effect that may be explained by its slightly higher affinity for uPAR than wild-type uPA (Hamelin et al., 1993). The relocalisation of focal contacts, formation of abundant new actin rich structures, increased migratory speed, polarisation and chemotaxis of cells induced by both EGF and uPA were indicative of their signalling through the small Rho GTPases and N-WASP (Allen et al., 1998; Miki et al., 1998; Ridley et al., 1992; Rohatgi et al., 1999). The concentrations of EGF or uPA that induced maximal chemotactic and migratory responses also stimulated maximal levels of Rho GTPase activity. The temporal profiles of Cdc42, Rac1 and N-WASP activation in uPA and EGF-stimulated cells correlated with the formation of their associated cytoskeletal structures. uPA and EGF both stimulated the formation of N-WASP/F-actin rich membrane ruffles and lamellipodia over the same time course as the initiation of the migratory response and sustained Rac1 activation (after 3-30 minutes stimulation). Cdc42 was rapidly activated by EGF, sustained at modest levels for up to 30 minutes and associated with latent translocation of N-WASP to the cytoskeleton (after 10-30 minutes stimulation) and microspike production in only few cells. Cdc42 activation in response to uPA was also rapid but transient and occurred directly in concert with the translocation of N-WASP to the cytoskeleton and formation of abundant microspikes (after only 1-3 minutes stimulation). Similar microspike production induced by uPA-uPAR signalling was observed in vascular smooth muscle cells (Degryse et al., 1999). Although uPAR binding to vitronectin stimulated lamellipodial protrusions through Rac1 activation, microspike formation or Cdc42 activation was not detected in an uPAR overexpression model (Kjoller and Hall, 2001). This contrary finding may have several explanations. Signal transduction molecules recruited by activated uPAR could be cell-type specific or different uPAR ligands could stimulate distinct cytoskeletal changes by preferential activation of specific signal transduction pathways, as suggested by Degryse et al. (Degryse et al., 2001). It may be that overexpression of uPAR by transfection results in elevated and sustained Rac1 activation, which suppresses Cdc42 activation and associated cytoskeletal rearrangements. The later possibility could result from the ability of small Rho GTPases to positively or negatively regulate each others activity during cell migration (Kjoller and Hall, 1999).

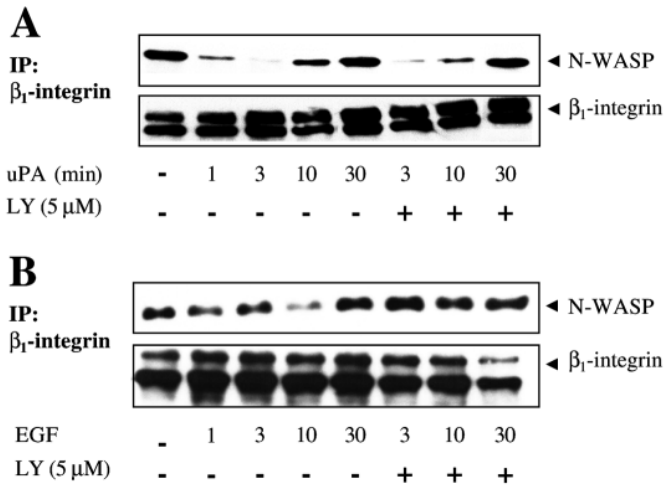

Fig. 10. PI3K-independent activation of N-WASP by uPA involves its disassociation from β_1-integrin. (A,B) β_1-integrin immunoprecipitates were separated on 10% gels and immunoblotted for N-WASP. (A) Cells stimulated with 10 nM uPA for 1-30 minutes±LY 294002 (5 μM). (B) Cells stimulated with 10 ng/ml EGF for 1-30 minutes±LY 294002. The results are representative of three experiments.

The involvement of PI3K in activation of GEFs for the small Rho GTPases, cytoskeletal rearrangements and chemotaxis (Arrieumerlou et al., 1998; Han et al., 1998; Hirsch et al., 2000; Li et al., 2000; Reif et al., 1996) led us to consider whether uPA-uPAR chemotactic signalling utilized PI3K for the activation of the small Rho GTPases. PI3K is suggested to act as an upstream effector for Rac1, and in some cases for Cdc42, in several growth factor and chemoattractant stimulated pathways (Banyard et al., 2000; Benard et al., 1999; Hawkins et al., 1995; Hooshmand-Jones, 2000; Ma et al., 1998). Recent studies by us and others have further confirmed that activation of specific PI3K p110 catalytic subunit isoforms in breast carcinoma cells is necessary for EGF-induced cytoskeletal changes (Hill et al., 2000) and chemotaxis (Sawyer et al., submitted for publication). uPA and EGF signalling through PI3K in MDA MB 231 cells was evident through their ability to stimulate Akt phosphorylation that was sensitive to inhibition by LY 294002. As predicted, Cdc42 activation, Rac1 activation, lamellipodial protrusion and chemotaxis stimulated by EGF were totally dependent on PI3K activity. Surprisingly we found that PI3K activity was not necessary for the vast majority of uPA-stimulated responses. Inhibition of PI3K had no effect on Cdc42 or Rac1 activation, chemotaxis or speed of cell movement.

What are the different mechanism(s) for PI3K-independent and PI3K-dependent activation of Cdc42 and Rac1 by uPA and EGF? Vav2 seemed a likely candidate GEF for differential upstream signalling to Cdc42 and Rac1 via uPA and EGF. Evidence from studies in HEK293 and fibroblast cell lines suggested that growth factor receptors signal via phosphorylation of Vav2 to activate the Rho GTPases Cdc42, Rac1 and RhoA (Liu and Burridge, 2000). However activation of Rho GTPases Cdc42, Rac1 and RhoA in response to β_1-integrin activation was found to be independent of Vav2 activation (Liu and Burridge, 2000). Despite successful Vav2 immunoprecipitation from MDA MB 231 cells, we could not detect altered tyrosine phosphorylation in response to either EGF or uPA (J.S., unpublished). This suggests that neither EGF nor uPA activates Vav2 in this cell line. However, differential signalling through other GEFs could underlie PI3K-dependent/independent activation of Rho GTPases by EGF and uPA.

PI3K-dependent signalling by uPA to the actin cytoskeleton was evident in MB MDA 231 cells. LY 294002 partially inhibited uPA-induced microspikes, an effect that correlated with a partial decrease in N-WASP localisation to the cytoskeletal fraction. Therefore, PI3K-dependent and PI3K-independent activation of N-WASP can activate microspike production in response to uPA. However, lamellipodia formation and Rho GTPase activation in response to uPA was unaffected by LY 294002, which is consistent with the lack of effect of PI3K inhibition on uPA-induced polarisation and chemotaxis. PI3K-independent N-WASP activation by uPA probably occurs through PI3K-independent activation of Cdc42/Rac1, whereas PI3K-dependent activation of this member of the WASP family may involve direct interaction of p85α with its polyproline region (Banin et al., 1996; Finan et al., 1996) or through other effector interactions. Nevertheless, it should be appreciated that our results indicate 'PI3K-dependent' N-WASP activation is not necessary for uPA-induced chemotaxis, whereas 'PI3K-independent' N-WASP activation is sufficient for uPA-induced chemotaxis.

A recently proposed mechanism for the promotion of vascular smooth muscle cell migration by uPA involved PI3K activation (Kusch et al., 2000). A similar mechanism was not apparent in MDA MB 231 breast carcinoma cells. Kusch et al. based the requirement of p110 PI3K catalytic activity in the migratory response to uPA on results from experiments using very high concentrations of LY 294002 (50 μM) and wortmannin (200 nM) (Kusch et al., 2000). Both inhibitors lose specificity for PI3K and inhibit kinases in other signalling pathways at such high concentrations (Vanhaesebroeck and Waterfield, 1999). In two recent reports, it was suggested that the p85 regulatory subunit of class 1A PI3Ks binds to and activates Cdc42 with no requirement for p110 catalytic activity (Hill et al., 2001; Jimenez et al., 2000). A similar interaction could explain the involvement of Tyk2-p85 in migration induced by uPA in vascular smooth muscle cells (Kusch et al., 2000). A similar mechanism could also exist in MDA MB 231 cells.

The involvement of β_1-integrins in chemotaxis and cytoskeletal reorganisation in MDA MB 231 cells stimulated by uPA was confirmed by several findings. Firstly, stimulation of cells with uPA resulted in re-distribution of focal complexes containing β_1-integrins. Secondly, a β_1-integrin blocking antibody inhibited chemotaxis towards uPA, and this correlated with inhibition of Cdc42/Rac1 activation. However, the inhibitory effects of anti-β_1-integrin on chemotaxis and activation of small GTPases was apparent in EGF-stimulated cells, and so it was not an uPAR-specific effect. However, an uPA–uPAR-specific role for β_1-integrins was identified and appears to be part of the mechanism involved in PI3K-independent activation of N-WASP. An interaction between β_1-integrins and N-WASP was fully disrupted upon uPA stimulation. This effect was rapid and transient (occurring after 1 minute uPA stimulation), in concert with the activation of Cdc42, and was not sensitive to inhibition by LY 294002. In

contrast, the effect of EGF on the interaction between β_1-integrins and N-WASP was far less dramatic and entirely PI3K dependent, being a latent and partial response (occurring after 10 minutes stimulation) and sensitive to inhibition by LY 294002. The transient nature of the disassociation of β_1-integrins and N-WASP induced by uPA indicates it may well have a role in the initiation of N-WASP activation. It remains to be determined whether the association of β_1-integrins with N-WASP occurs through a direct interaction between the two molecules or whether intermediate proteins recruit N-WASP to the complex. The exact mechanism of this molecular interaction and its disruption upon uPAR ligation awaits further characterisation. Nevertheless, this potential mechanism for N-WASP activation could endow cells with the ability to respond to specific chemotactic cues in the absence of PI3K activity.

The authors were funded by the Association for International Cancer Research and the Wellcome Trust.

References

Adams, J. C. (2001). Cell-matrix contact structures. *Cell. Mol. Life Sci.* **58**, 371-392.

Allen, W. E., Jones, G. E., Pollard, J. W. and Ridley, A. J. (1997). Rho, Rac and Cdc42 regulate actin organization and cell adhesion in macrophages. *J. Cell Sci.* **110**, 707-720.

Allen, W. E., Zicha, D., Ridley, A. J. and Jones, G. E. (1998). A role for Cdc42 in macrophage chemotaxis. *J. Cell Biol.* **141**, 1147-1157.

Andreasen, P. A., Kjoller, L., Christensen, L. and Duffy, M. J. (1997). The urokinase-type plasminogen activator system in cancer metastasis: a review. *Int. J. Cancer* **72**, 1-22.

Arrieumerlou, C., Donnadieu, E., Brennan, P., Keryer, G., Bismuth, G., Cantrell, D. and Trautmann, A. (1998). Involvement of phosphoinositide 3-kinase and Rac in membrane ruffling induced by IL-2 in T cells. *Eur. J. Immunol.* **28**, 1877-1885.

Banin, S., Truong, O., Katz, D. R., Waterfield, M. D., Bricknell, P. M. and Gout, I. (1996). Wiskott-Aldrich syndrome protein (WASp) is a binding partner for c-Src family protein-tyrosine kinases. *Curr. Biol.* **6**, 981-988.

Banyard, J., Anand-Apte, B., Symons, M. and Zetter, B. R. (2000). Motility and invasion are differentially modulated by Rho family GTPases. *Oncogene* **19**, 580-591.

Benard, V., Bohl, B. P. and Bokoch, G. M. (1999). Characterization of Rac and Cdc42 activation in chemoattractant-stimulated human neutrophils using a novel assay for active GTPases. *J. Biol. Chem.* **274**, 13198-13204.

Bohuslav, J., Horejsi, V., Hansmann, C., Stockl, J., Weidle, U. H., Majdic, O., Bartke, I., Knapp, W. and Stockinger, H. (1995). Urokinase plasminogen-activator receptor, beta-2-integrins, and src-kinases within a single receptor complex of human monocytes. *J. Exp. Med.* **181**, 1381-1390.

Busso, N., Masur, S. K., Lazega, D., Waxman, S. and Ossowski, L. (1994). Induction of cell-migration by prourokinase binding to its receptor – possible mechanism for signal-transduction in human epithelial-cells. *J. Cell Biol.* **126**, 259-270.

Carriero, M. V., Del Vecchio, S., Capozzoli, M., Franco, P., Fontana, L., Zannetti, A., Botti, G., D'Aiuto, G., Salvatore, M. and Stoppelli, M. P. (1999). Urokinase receptor interacts with alpha(v)beta(5) vitronectin receptor, promoting urokinase-dependent cell migration in breast cancer. *Cancer Res.* **59**, 5307-5314.

Chiaradonna, F., Fontana, L., Iavarone, C., Carriero, M. V., Scholz, G., Barone, M. V. and Stoppelli, M. P. (1999). Urokinase receptor-dependent and –independent p56/59(hck) activation state is a molecular switch between myelomonocytic cell motility and adherence. *EMBO J.* **18**, 3013-3023.

Degryse, B., Resnati, M., Rabbani, S. A., Villa, A., Fazioli, F. and Blasi, F. (1999). Src-dependence and pertussis toxin sensitivity of urokinase receptor-dependent chemotaxis and cytoskeleton reorganization in rat smooth muscle cells. *Blood* **94**, 649-662.

Degryse, B., Orlando, S., Resnati, M., Rabbani, S. A. and Blasi, F. (2001). Urokinase/urokinase receptor and vitronectin/alpha(v)beta(3) integrin induce chemotaxis and cytoskeleton reorganization through different signaling pathways. *Oncogene* **20**, 2032-2043.

Fawcett, J. and Pawson, T. (2000). Signal transduction – N-WASP regulation – the sting in the tail. *Science* **290**, 725-726.

Fibbi, G., Caldini, R., Chevanne, M., Pucci, M., Schiavone, N., Morbidelli, L., Parenti, A., Granger, H. J., Del Rosso, M. and Ziche, M. (1998). Urokinase-dependent angiogenesis in vitro and diacylglycerol production are blocked by antisense oligonucleotides against the urokinase receptor. *Lab. Invest.* **78**, 1109-1119.

Finan, P. M., Soames, C. J., Wilson, L., Nelson, D. L., Stewart, D. M., Truong, O., Hsuan, J. J. and Kellie, S. (1996). Identification of regions of the Wiskott-Aldrich syndrome protein responsible for association with selected Src homology 3 domains. *J. Biol. Chem.* **271**, 26291-26295.

Foekens, J. A., Peters, H. A., Look, M. P., Portengen, H., Schmitt, M., Kramer, M. D., Brunner, N., Janicke, F., Gelder, M. E. M., Henzen-Logmans, S. C. et al. (2000). The urokinase system of plasminogen activation and prognosis in 2780 breast cancer patients. *Cancer Res.* **60**, 636-643.

Hamelin, J., Sarmientos, P., Orsini, G. and Galibert, F. (1993). Implication of cysteine residues in the activity of single-chain urokinase-plasminogen activator. *Biochem. Biophys. Res. Commun.* **194**, 978-985.

Han, J. W., Luby-Phelps, K., Das, B., Shu, X. D., Xia, Y., Mosteller, R. D., Krishna, U. M., Falck, J. R., White, M. A. and Broek, D. (1998). Role of substrates and products of PI3-kinase in regulating activation of Rac-related guanosine triphosphatases by Vav. *Science* **279**, 558-560.

Haugh, J. M., Codazzi, F., Teruel, M. and Meyer, T. (2000). Spatial sensing in fibroblasts mediated by 3′ phosphoinositides. *J. Cell Biol.* **151**, 1269-1279.

Hawkins, P. T., Eguinoa, A., Qiu, R. G., Stokoe, D., Cooke, F. T., Walters, R., Wennstrom, S., Claessonwelsh, L., Evans, T., Symons, M. and Stephens, L. (1995). PDGF stimulates an increase in GTP-Rac via activation of phosphoinositide 3-kinase. *Curr. Biol.* **5**, 393-403.

Hebert, C. A. and Baker, J. B. (1988). Linkage of extracellular plasminogen-activator to the fibroblast cystoskeleton – colocalization of cell-surface urokinase with vinculin. *J. Cell Biol.* **106**, 1241-1247.

Hill, K., Welti, S., Yu, J. H., Murray, J. T., Yip, S. C., Condeelis, J. S., Segall, J. E. and Backer, J. M. (2000). Specific requirement for the p85-p110 alpha phosphatidylinositol 3-kinase during epidermal growth factor-stimulated actin nucleation in breast cancer cells. *J. Biol. Chem.* **275**, 3741-3744.

Hill, K. M., Huang, Y., Yip, S. C., Yu, J., Segall, J. E. and Backer, J. M. (2001). N-terminal domains of the class Ia phosphoinositide 3-kinase regulatory subunit play a role in cytoskeletal but not mitogenic signaling. *J. Biol. Chem.* **276**, 16374-16378.

Hirsch, E., Katanaev, V. L., Garlanda, C., Azzolino, O., Pirola, L., Silengo, L., Sozzani, S., Mantovani, A., Altruda, F. and Wymann, M. P. (2000). Central role for G protein-coupled phosphoinositide 3-kinase gamma in inflammation. *Science* **287**, 1049-1053.

HooshmandRad, R., ClaessonWelsh, L., Wennstrom, S., Yokote, K., Siegbahn, A. and Heldin, C. H. (1997). Involvement of phosphatidylinositide 3′-kinase and Rac in platelet-derived growth factor-induced actin reorganization and chemotaxis. *Exp. Cell Res.* **234**, 434-441.

Jimenez, C., Portela, R. A., Mellado, M., Rodriguez-Frade, J. M., Collard, J., Serrano, A., Martinez, A., Avila, J. and Carrera, A. C. (2000). Role of the PI3K regulatory subunit in the control of actin organization and cell migration. *J. Cell Biol.* **151**, 249-261.

Jones, G. E. (2000). Cellular signaling in macrophage migration and chemotaxis. *J. Leukocyte Biol.* **68**, 593-602.

Jones, G. E., Ridley, A. J. and Zicha, D. (2000). Rho GTPases and cell migration: Measurement of macrophage chemotaxis. *Regulators and Effectors of Small GTPases, Pt D* **325**, 449-462.

Kim, A. S., Kakalis, L. T., Abdul-Manan, M., Liu, G. A. and Rosen, M. K. (2000). Autoinhibition and activation mechanisms of the Wiskott-Aldrich syndrome protein. *Nature* **404**, 151-158.

Kim, H. and Muller, W. J. (1999). The role of the epidermal growth factor receptor family in mammary tumorigenesis and metastasis. *Exp. Cell Res.* **253**, 78-87.

Kjoller, L. and Hall, A. (1999). Signaling to Rho GTPases. *Exp. Cell Res.* **253**, 166-179.

Kjoller, L. and Hall, A. (2001). Rac mediates cytoskeletal rearrangements and increased cell motility induced by urokinase-type plasminogen activator receptor binding to vitronectin. *J. Cell Biol.* **152**, 1145-1157.

Kolluri, R., Tolias, K. F., Carpenter, C. L., Rosen, F. S. and Kirchhausen, T. (1996). Direct interaction of the Wiskott-Aldrich syndrome protein with the GTPase Cdc42. *Proc. Nat. Acad. Sci. USA.* **93**, 5615-5618.

Kozma, R., Ahmed, S., Best, A. and Lim, L. (1995). The Ras-related protein

Cdc42hs and bradykinin promote formation of peripheral actin microspikes and filopodia in swiss 3T3 fibroblasts. *Mol. Cell. Biol.* **15**, 1942-1952.

Kusch, A., Tkachuk, S., Haller, H., Dietz, R., Gulba, D. C., Lipp, M. and Dumler, I. (2000). Urokinase stimulates human vascular smooth muscle cell migration via a phosphatidylinositol 3-kinase-Tyk2 interaction. *J. Biol. Chem.* **275**, 39466-39473.

Li, Z., Jiang, H. P., Xie, W., Zhang, Z. C., Smrcka, A. V. and Wu, D. Q. (2000). Roles of PLC-beta 2 and -beta 3 and PI3K gamma in chemoattractant-mediated signal transduction. *Science* **287**, 1046-1049.

Liotta, L. A. and Kohn, E. C. (2001). The microenvironment of the tumour-host interface. *Nature* **411**, 375-379.

Liu, B. P. and Burridge, K. (2000). Vav2 activates Rac1, Cdc42, and RhoA downstream from growth factor receptors but not beta 1 integrins. *Mol. Cell. Biol.* **20**, 7160-7169.

Ma, A. D., Metjian, A., Bagrodia, S., Taylor, S. and Abrams, C. S. (1998). Cytoskeletal reorganization by G protein-coupled receptors is dependent on phosphoinositide 3-kinase gamma, a Rac guanosine exchange factor, and Rac. *Mol. Cell. Biol.* **18**, 4744-4751.

Machesky, L. M. and Hall, A. (1997). Role of actin polymerization and adhesion to extracellular matrix in Rac- and Rho-induced cytoskeletal reorganization. *J. Cell Biol.* **138**, 913-926.

Mardia, K. V. (1972). *Statistics of Directional Data*, pp. 1-357. New York, Academic Press.

Miki, H., Miura, K. and Takenawa, T. (1996). N-WASP, a novel actin-depolymerizing protein, regulates the cortical cytoskeletal rearrangement in a PIP2-dependent manner downstream of tyrosine kinases. *EMBO J.* **15**, 5326-5335.

Miki, H., Sasaki, T., Takai, Y. and Takenawa, T. (1998). Induction of filopodium formation by a WASP-related actin-depolymerizing protein N-WASP. *Nature* **391**, 93-96.

Miki, H. and Takenawa, T. (1998). Direct binding of the verprolin-homology domain in N-WASP to actin is essential for cytoskeletal reorganization. *Biochem. Biophys. Res. Commun.* **243**, 73-78.

Millard, T. H. and Machesky, L. M. (2001). The Wiskott-Aldrich syndrome protein (WASP) family. *Trends Biochem. Sci.* **26**, 198-199.

Moghal, N. and Sternberg, P. W. (1999). Multiple positive and negative regulators of signaling by the EGF-receptor. *Curr. Opin. Cell Biol.* **11**, 190-196.

Muller, A., Homey, B., Soto, H., Ge, N., Catron, D., Buchanan, M. E., McClanahan, T., Murphy, E., Yuan, W., Wagner, S. N. et al. (2001). Involvement of chemokine receptors in breast cancer metastasis. *Nature* **410**, 50-56.

Mullins, R. D. and Machesky, L. M. (2000). Actin assembly mediated by Arp2/3 complex and WASP family proteins. *Regulators and Effectors of Small GTPases, Pt D* **325**, 214-237.

Nguyen, D. H. D., Catling, A. D., Webb, D. J., Sankovic, M., Walker, L. A., Somlyo, A. V., Weber, M. J. and Gonias, S. L. (1999). Myosin light chain kinase functions downstream of Ras/ERK to promote migration of urokinase-type plasminogen activator- stimulated cells in an integrin-selective manner. *J. Cell Biol.* **146**, 149-164.

Nguyen, D. H. D., Webb, D. J., Catling, A. D., Song, Q., Dhakephalkar, A., Weber, M. J., Ravichandran, K. S. and Gonias, S. L. (2000). Urokinase-type plasminogen activator stimulates the Ras/extracellular signal-regulated kinase (ERK) signaling pathway and MCF-7 cell migration by a mechanism that requires focal adhesion kinase, Src, and Shc – Rapid dissociation of Grb2/Sos-Shc complex is associated with the transient phosphorylation of ERK in urokinase-treated cells. *J. Biol. Chem.* **275**, 19382-19388.

Nobes, C. D. and Hall, A. (1995). Rho, Rac, and Cdc42 GTPases regulate the assembly of multimolecular focal complexes associated with actin stress fibers, lamellipodia, and filopodia. *Cell* **81**, 53-62.

Nobes, C. D. and Hall, A. (1999). Rho GTPases control polarity, protrusion, and adhesion during cell movement. *J. Cell Biol.* **144**, 1235-1244.

Ossowski, L. and Aguirre-Ghiso, J. A. (2000). Urokinase receptor and integrin partnership: coordination of signaling for cell adhesion, migration and growth. *Curr. Opin. Cell Biol.* **12**, 613-620.

Preissner, K. T., Kanse, S. M. and May, A. E. (2000). Urokinase receptor: a molecular organizer in cellular communication. *Curr. Opin. Cell Biol.* **12**, 621-628.

Reif, K., Nobes, C. D., Thomas, G., Hall, A. and Cantrell, D. A. (1996). Phosphatidylinositol 3-kinase signals activate a selective subset of Rac/Rho-dependent effector pathways. *Curr. Biol.* **6**, 1445-1455.

Resnati, M., Guttinger, M., Valcamonica, S., Sidenius, N., Blasi, F. and Fazioli, F. (1996). Proteolytic cleavage of the urokinase receptor substitutes for the agonist-induced chemotactic effect. *EMBO J.* **15**, 1572-1582.

Ridley, A. J. and Hall, A. (1992). The small GTP-binding protein Rho regulates the assembly of focal adhesions and actin stress fibers in response to growth-factors. *Cell* **70**, 389-399.

Ridley, A. J., Paterson, H. F., Johnston, C. L., Diekmann, D., And Hall, A. (1992). The small GTP-binding protein Rac regulates growth-factor induced membrane ruffling. *Cell* **70**, 401-410.

Ridley, A. J., Allen, W. E., Peppelenbosch, M. and Jones, G. E. (1999). Rho family proteins and cell migration. *Biochem. Soc. Symp.* **65**, 111-123.

Rohatgi, R., Ma, L., Miki, H., Lopez, M., Kirchhausen, T., Takenawa, T. and Kirschner, M. W. (1999). The interaction between N-WASP and the Arp2/3 links Cdc42-dependent signals to actin assembly. *Cell* **97**, 221-231.

Rottner, K., Hall, A. and Small, J. V. (1999). Interplay between Rac and Rho in the control of substrate contact dynamics. *Curr. Biol.* **9**, 640-648.

Sander, E. E., van Delft, S., ten Klooster, J. P., Reid, T., van der Kammen, R. A., Michiels, F. and Collard, J. G. (1998). Matrix-dependent Tiam1/Rac signaling in epithelial cells promotes either cell-cell adhesion or cell migration and is regulated by phosphatidylinositol 3-kinase. *J. Cell Biol.* **143**, 1385-1398.

Schmitt, M., Wilhelm, O. G., Reuning, U., Kruger, A., Harbeck, N., Lengyel, E., Graeff, H., Gansbacher, B., Kessler, H., Burgle, M., Sturzebecher, J., Sperl, S. and Magdolen, V. (2000). The urokinase plasminogen activator system as a novel target for tumour therapy. *Fibrinolysis & Proteolysis* **14**, 114-132.

Schmitz, A. A. P., Govek, E. E., Bottner, B. and Van Aelst, L. (2000). Rho GTPases: Signaling, migration, and invasion. *Exp. Cell Res.* **261**, 1-12.

She, H. Y., Rockow, S., Tang, J., Nishimura, R., Skolnik, E. Y., Chen, M., Margolis, B. and Li, W. (1997). Wiskott-Aldrich syndrome protein is associated with the adapter protein Grb2 and the epidermal growth factor receptor in living cells. *Mol. Biol. Cell* **8**, 1709-1721.

Simon, D. I., Wei, Y., Zhang, L., Rao, N. K., Xu, H., Chen, Z. P., Liu, Q. M., Rosenberg, S. and Chapman, H. A. (2000). Identification of a urokinase receptor-integrin interaction site – Promiscuous regulator of integrin function. *J. Biol. Chem.* **275**, 10228-10234.

Sitrin, R. G., Todd, R. F., Petty, H. R., Brock, T. G., Shollenberger, S. B., Albrecht, E. and Gyetko, M. R. (1996). The urokinase receptor (CD87) facilitates CD11b/CD18-mediated adhesion of human monocytes. *J. Clin. Invest.* **97**, 1942-1951.

Symons, M., Derry, J. M. J., Karlak, B., Jiang, S., Lemahieu, V., McCormick, F., Francke, U. and Abo, A. (1996). Wiskott-Aldrich syndrome protein, a novel effector for the GTPase CDC42Hs, is implicated in actin polymerization. *Cell* **84**, 723-734.

Takenawa, T. and Miki, H. (2001). WASP and WAVE family proteins: key molecules for rapid rearrangement of cortical actin filaments and cell movement. *J. Cell Sci.* **114**, 1801-1809.

Vanhaesebroeck, B. and Waterfield, M. D. (1999). Signaling by distinct classes of phosphoinositide 3-kinases. *Exp. Cell Res.* **253**, 239-254.

Vanhaesebroeck, B., Jones, G. E., Allen, W. E., Zicha, D., Hooshmand-Rad, R., Sawyer, C., Wells, C., Waterfield, M. D. and Ridley, A. J. (1999). Distinct PI(3)Ks mediate mitogenic signalling and cell migration in macrophages. *Nat. Cell Biol.* **1**, 69-71.

Webb, S. E., Pollard, J. W. and Jones, G. E. (1996). Direct observation and quantification of macrophage chemoattraction to the growth factor CSF-1. *J. Cell Sci.* **109**, 793-803.

Wei, Y., Lukashev, M., Simon, D. I., Bodary, S. C., Rosenberg, S., Doyle, M. V. and Chapman, H. A. (1996). Regulation of integrin function by the urokinase receptor. *Science* **273**, 1551-1555.

Wells, A., Gupta, K., Chang, P., Swindle, S., Glading, A. and Shiraha, H. (1998). Epidermal growth factor receptor-mediated motility in fibroblasts. *Microscopy Res. Technique* **43**, 395-411.

Xue, W., Mizukami, I., Todd, R. F., III and Petty, H. R. (1997). Urokinase-type plasminogen activator receptors associate with beta1 and beta3 integrins of fibrosarcoma cells: dependence on extracellular matrix components. *Cancer Res.* **57**, 1682-1689.

Yebra, M., Goretzki, L., Pfeifer, M. and Mueller, B. M. (1999). Urokinase-type plasminogen activator binding to its receptor stimulates tumor cell migration by enhancing integrin-mediated signal transduction. *Exp. Cell Res.* **250**, 231-240.

Zicha, D., Dunn, G. A. and Brown, A. F. (1991). A new direct-viewing chemotaxis chamber. *J. Cell Sci.* **99**, 769-775.